Transport of a heated granular gas in a washboard potential

Giulio Costantini
Dipartimento di Fisica, Università di Camerino, Via Madonna delle Carceri, 68032 Camerino, Macerata, Italy

Fabio Cecconi[a)]
INFM Center for Statistical Mechanics and Complexity, P.le Aldo Moro 2, 00185 Rome (Italy) and Institute for Complex Systems, CNR, Via dei Taurini 19, 00185 Rome (Italy)

Umberto Marini-Bettolo-Marconi
Dipartimento di Fisica, Università di Camerino, Via Madonna delle Carceri, 68032 Camerino, Macerata, Italy

(Received 1 August 2006; accepted 6 October 2006; published online 28 November 2006)

We study numerically the motion of a one dimensional array of Brownian particles in a washboard potential, driven by an external stochastic force and interacting via short range repulsive forces. In particular, we investigate the role of instantaneous elastic and inelastic collisions on the system dynamics and transport. The system displays a locked regime, where particles may move only via activated processes and a running regime where particles drift along the direction of the applied field. By tuning the value of the friction parameter controlling the Brownian motion we explore both the overdamped dynamics and the underdamped dynamics. In the two regimes we considered the mobility and the diffusivity of the system as functions of the tilt and other relevant control parameters such as coefficient of restitution, particle size, and total number of particles. We find that while in the overdamped regime the results for the interacting systems present similarities with the known noninteracting case, in the underdamped regime the inelastic collisions determine a rich variety of behaviors among which is an unexpected enhancement of the inelastic diffusion. © *2006 American Institute of Physics*. [DOI: 10.1063/1.2378873]

I. INTRODUCTION

A large class of phenomena in biology, chemistry, engineering, and physics occurs via the transport of particles driven along periodic substrates by an external bias. These phenomena include polymer diffusion at interfaces,[1] motion of fluxons in superconductors containing a periodic arrangement of defects,[2,3] adsorption on crystal surfaces,[4] superionic conduction,[5] motion of molecular motors along microtubules,[6] granular flows on rough inclined substrates,[7–11] or in a narrow pipe.[12]

The study of transport properties of granular systems represents an open issue in statistical mechanics of considerable interest and difficulty in view of the continuous energy dissipation caused by particle inelastic interactions.[13] In this perspective, we consider a simple model consisting of a granular fluid moving on a tilted rough substrate, which may favor clustering and jamming behaviors.

In our formulation, a granular system is a large number of particles (grains) colliding with one another and losing a little energy in each collision.[14–18] If such a system is shaken to keep it in motion its dynamics resembles that of fluids as the grains move randomly.[19]

We carry out a comparative study of the behavior of three models: the inelastic particle system (IPS), the elastic particle system (EPS), and finally the noninteracting system or independent Brownian particles (IBP) to understand how the interactions influence the collective transport. The absence of interactions between particles makes the basic phenomenology of the IBP well understood. It reduces, indeed, to the motion of a single particle in a force field resulting from the interplay between a constant force F, such as gravity or electric field, a spatially periodic force, simulating the presence of a rough substrate, a viscous force accounting for the friction, and a noise term, representing thermal fluctuations.[20] The scenario is the following: particles diffuse with a bias in the direction of the steady force F with an average velocity v_m which is an increasing function of the applied load F. However, when the load is below a critical value, F_c, and the noise sufficiently small, the average velocity tends to zero. In other words the particles remain locked in the minima of the periodic potential. On the other hand, above the threshold, F_c, the particles may travel from one minimum to the other along the tilt direction. The critical value, F_c, depends on roughness, friction, and temperature. According to the value of the friction coefficient two different scenarios may be observed. In the so called overdamped limit, F_c occurs only when the tilt is such that the local minima completely disappear. In the opposite limit, i.e., in the underdamped regime, the particles may overcome many barriers even for low values of F at which the potential still displays local minima. In fact, the particles may cross a barrier, provided their gain in potential energy, to go from one

[a)]Electronic mail: cecconif@roma1.infn.it

minimum to the next, exceeds the energy dissipated along this pathway. In the underdamped limit the exact value of F_c depends on the temperature.

Two indicators may serve to characterize the collective transport properties of the system, the mobility μ and the diffusion constant D. The former relates the average velocity to the tilt F according to $\langle v\rangle=\mu(F)F$. The latter measures the average spreading of particles:

$$R(t)=\langle[x(t)-\langle x_{\mathrm{c.m.}}(t)\rangle]^2\rangle. \tag{1}$$

The average is meant over the thermal noise realizations. In all the cases where $R(t)$ asymptotically grows linearly in time, we can identify the normal diffusion constant D defined as the slope of the law

$$R(t)\sim 2Dt$$

that generally is computed numerically through simulations of the system evolution. The study of the dependence of μ and D on F and other system parameter is necessary to determine the efficiency of the transport, i.e., the ratio between drift and spreading of a swarm of particles.

A detailed theory capable of describing the behavior of the IBP for arbitrary values of the damping has been developed by Risken[20] and Coffey *et al.*[21] who derived an analytical expression for the mobility μ as a function of noise level, tilting force, and substrate characteristics. A closed formula for the diffusion coefficient exists only for the overdamped situation.[22] It predicts the presence of a striking enhancement of D near a threshold, F_3, separating the locked from the running phase and corresponding to the disappearance of the local minima of the potential.

On the other hand, in the underdamped regime there is no analytic expression for D, but the enhancement of the diffusion coefficient occurs at a lower threshold, F_2,[20,23] due to the effect of inertia, and the phenomenon remains qualitatively similar.

The goal of the present paper is to consider the effects of interactions among particles on the transport properties in such systems. Specifically, we will address the following question: how do interactions occurring via elastic/inelastic hard-core collisions affect the mobility and the diffusion of an assembly of particles? This issue is particular relevant in one dimension where a repulsive hard-core interaction inhibits the particles to pass each other; this constraint is known to influence dramatically the dynamics of a group of particles. As an example, we can mention the anomalous self-diffusion in single file systems.[24–26]

We focus our dynamical approach only on exploring the effects of repulsive interactions via impulsive contact collisions. We consider two possibilities, energy conserving collisions and dissipative inelastic collisions. Both situations are still largely unexplored in systems with washboard potentials and display nontrivial behaviors, as we shall illustrate. For instance, the mutual repulsion between the particles induces dynamical correlations which may favor or hinder their motions: it can promote their exit from a potential well via energetic collisions or, on the contrary, it can prevent a jump to a given site when this is too crowded. In addition, the granular temperature, defined as the average kinetic energy per particle, in inelastic systems is in general lower than the corresponding temperature of elastic systems. Therefore, the transport, occurring via thermally activated processes across substrate barriers, is expected to be less efficient for inelastic particles.[27] Then few questions can be addressed. Does the diffusivity D present an enhancement analogous to that of noninteracting systems? Does the threshold locked to running occur at larger values of the tilt? In the following, we answer the questions by examining a variety of situations and analyzing the overdamped and the underdamped regimes separately.

The paper is organized as follows. In Sec. II, we present the model and discuss the contact elastic/inelastic interaction with their main implication in the system dynamics. In Sec. III, we analyze the results from the molecular dynamics (MD) simulations of the overdamped regime. In Sec. IV, we summarize the corresponding results for the underdamped regime discussing the salient differences with the overdamped case. Finally, conclusions are drawn in Sec. V.

II. MODEL

We consider a randomly driven granular gas, already introduced in previous works,[28] composed of N impenetrable hard rods of mass m and size σ moving on a line of length L in the presence of an external washboard potential. The overall dynamics of this gas is described by the Langevin equation for each rod,

$$m\frac{d^2x_i(t)}{dt^2}=-m\gamma\frac{dx_i(t)}{dt}+\xi_i(t)+\sum_{j\neq i}f_{ij}-\frac{d\Psi[x_i(t)]}{dx_i}+F, \tag{2}$$

that embodies four types of physical phenomena: friction with the surroundings, random accelerations due to external driving, inelastic collisions among the particles, and external time independent, but spatially varying, force. We model the first two effects by means of a stochastic bath with a viscous friction $-m\gamma\dot{x}_i$ and Gaussian random force, with zero average and covariance,

$$\langle\xi_i(t)\xi_j(t')\rangle=2m\gamma T\delta_{ij}\delta(t-t'), \tag{3}$$

satisfying a fluctuation-dissipation relation, with T proportional to the intensity of the stochastic driving.[29] The damping term fulfilling Einstein's relation renders the system stationary even in the absence of collisional dissipation and physically can represent the friction between the particles and the container. The interactions among the particles, indicated formally by $\Sigma_j f_{ij}$ in Eq. (2), amount to simple impulsive forces acting on the rod i due to the collisions with the neighboring particles j.[30–33] Thus a rod i performs, under the influence of the bath and collisions only, independent Brownian trajectories, unless it gets in contact with particle j, i.e., $|x_j-x_i|=\sigma$, at which point the velocities of the colliding pair (i,j) change instantaneously according to the inelastic rule

$$v_i'=v_i-\frac{1+\alpha}{2}(v_i-v_j),$$

$$v_j' = v_j + \frac{1+\alpha}{2}(v_i - v_j),$$

the prime indicating postcollisional variables and α the coefficient of restitution, with $0 \leqslant \alpha \leqslant 1$.

The total force, in Eq. (2), on each particle is supplemented by terms representing the presence of a constant external bias F and a periodic substrate generating a potential $\Psi(x)$, with period w and amplitude V_0,

$$\Psi(x) = -V_0 \cos(2\pi x/w). \tag{4}$$

A quantitative criterion to distinguish between an overdamped and an underdamped regime is provided by the dimensionless parameter $\Gamma = \gamma/\omega_0$, where

$$\omega_0 = \sqrt{\frac{1}{m}\left[\frac{d^2\Psi(x)}{dx^2}\right]_{\min}}$$

is the oscillation frequency at the potential minimum. If $\Gamma \gg 1$ the dynamics is overdamped, and in the opposite limit is underdamped.

As discussed by Borromeo and Marchesoni,[34,35] the present model is equivalent to considering the particles in a traveling potential, i.e., a periodic potential moving at speed c, which is related to the tilt force by the relation $F = m\gamma c$. Interestingly for speeds lower than a certain threshold the traveling wave has the capability of dragging the particles, a mechanism known as Stokes' drift.[36,37]

Thus, the system can equivalently describe the physics of a one dimensional granular gas where the periodic potential $\Psi(x)$ represents a series of compartments separated by walls, an experimental setup recently employed to study the clustering behavior of vibrated granular gases,[38,39] or the roughness of an inclined plane.[8,9]

III. NEARLY OVERDAMPED REGIME

We shall begin by considering the nearly overdamped regime ($\Gamma \simeq 2.1$), whose study is better understood because the system reaches a steady state rapidly due to the large value of the friction.

Our MD simulations were carried out by evolving an initial configuration, where the particles were all located in the central well without overlaps and their velocities were extracted from a Maxwell-Boltzmann distribution of temperature T. Each run involved $N=256$ particles of size $\sigma=1$ and mass $m=1$, with three different values of the coefficient of restitution, $\alpha=0.8$, 0.9, and 1.0, respectively. The substrate potential was characterized by wells of width $w=400\sigma$ and height $V_0=9.0$, in units of k_BT. Finally, the heat bath temperature has been chosen to be $T=1.0$ and $k_B=1$. The time is measured in units of $t_u=\sigma\sqrt{m/T}$. The friction coefficient is $\gamma=2/t_u$. The cyclic system studied has been taken to be of length $L=10^8 w$ so that it is virtually equivalent to a system with open boundary conditions. In this condition of high dilution, the global system density $\rho=N/L$ is extremely low; however, it is not a meaningful parameter, rather it is the initial density profile, characterized by the number of particles in a well $\rho_w=N/w$, that has a strong influence on the system behavior. Indeed, at the beginning of the evolution, the system needs to be packed enough to reach a not negligible collision rate. Only in the later stages of the simulations is a crossover observed toward the behavior of rarefied gases.

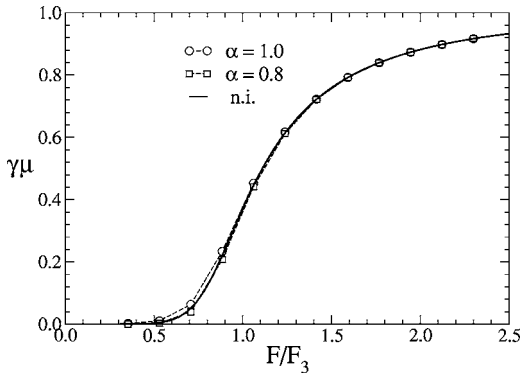

FIG. 1. Dimensionless mobility $\gamma\mu$ as a function of the rescaled external force F/F_3 ($F_3=2\pi V_0/w$) for $\alpha=1.0$ (circles) and $\alpha=0.8$ (squares) for a system with $N=256$ particles, temperature $T=1$, friction $\gamma=2/t_u$, and potential amplitude $V_0=9.0$, $\sigma=1$, $w/\sigma=400$. The system evolution is simulated for $t_{\max}=10\,000$ time units. The full line indicates the corresponding curve for the noninteracting particles obtained by the continued fraction method (Ref. 20).

At first sight, the MD simulations of the interacting system display a mobility quite similar to that of the noninteracting system: the curves $\gamma\mu$ vs F for elastic and inelastic hard-rod systems are shown in Fig. 1. In the same figure, we also plot the corresponding quantity relative to the IBP as calculated numerically by means of the continued fraction method.[20] However, a closer inspection reveals that differences do exist between the IBP and the interacting systems with different inelasticity α. Figure 2 shows the ratio of the mobilities of interacting systems to the mobility of the IBP. This ratio, for small values of the load, $F \ll F_3 = 2\pi V_0/w$, can be significantly different from 1, and more specifically the mobility of the EPS exceeds the mobility of the IBP, whereas the mobility of the IPS is lower. The reason for these differences can be found in the fact that contact interactions may change drastically, with respect to the IBP, the time that particles spend in a given potential minimum.

In more detail, these behaviors can be explained by recalling that two competing mechanisms contribute to the sys-

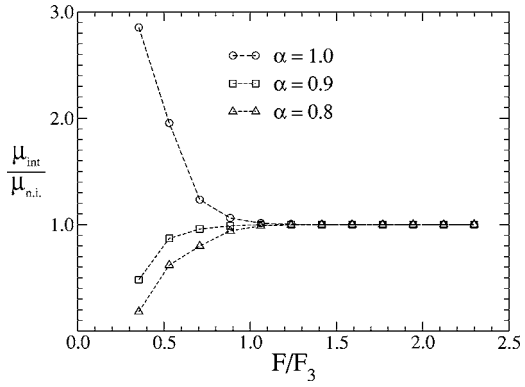

FIG. 2. The ratio between mobilities of interacting and noninteracting systems as a function of the rescaled external force F/F_3 ($F_3=2\pi V_0/w$) for $\alpha=1.0$ (circles), $\alpha=0.9$ (squares), and $\alpha=0.8$ (triangles). The remaining parameters are the same as in Fig. 1.

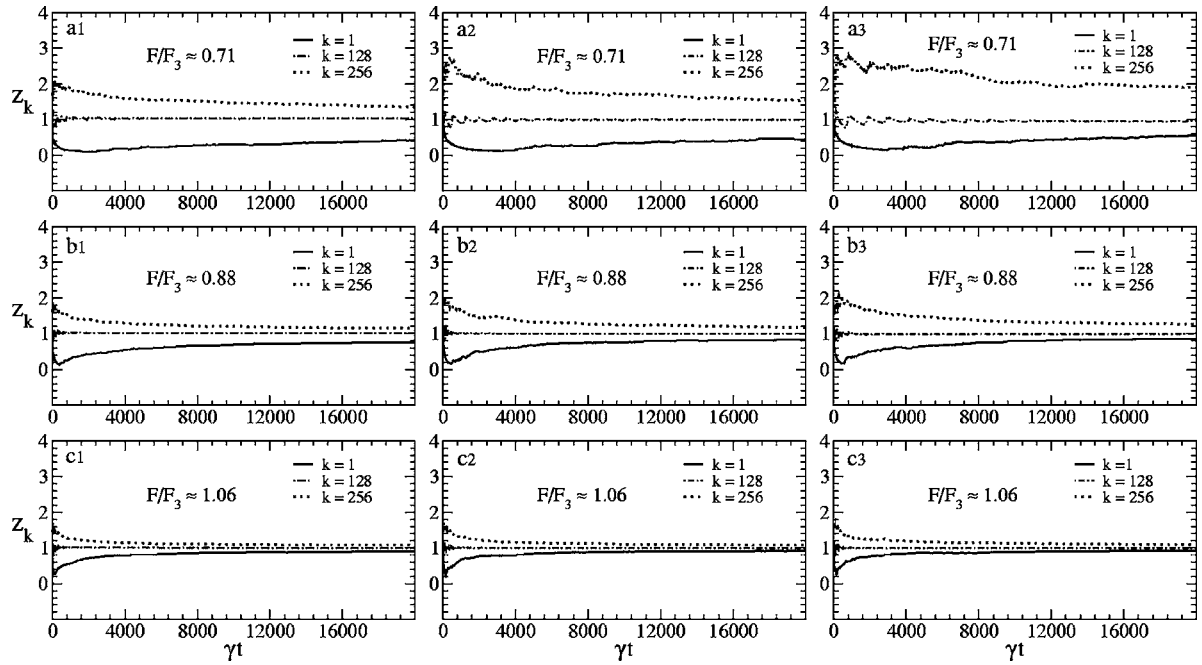

FIG. 3. Evolution of the normalized displacements from the initial position [see Eq. (5)] of the trajectories referring to tagged particles $k=1$ (full line), $k=128$ (broken line with dots), and $k=256$ (dots). The normalization is performed with respect to the displacement of the center of mass from its initial coordinate. The panels a1, a2, and a3 refer to rescaled forces $F/F_3 \simeq 0.71$, b1, b2, and b3 to $F/F_3 \simeq 0.88$, and finally c1, c2, and c3 to $F/F_3 \simeq 1.06$. The system contains $N=256$ particles. The coefficients of the restitution are $\alpha=1.0$ (in plots a1, b1, and c1), $\alpha=0.9$ (in plots a2, b2, and c2), and $\alpha=0.8$ (in plots a3, b3, and c3). Data are averaged over ten independent realizations and the remaining parameters are the same as in Fig. 1.

tem mobility: the excluded volume and the inelasticity. The first leads to an effective reduction of the barrier height and favors the escape from the wells, thus basically increasing the mobility. The second, instead, tends to decrease the average kinetic energy, rendering longer, on average, the time spent by the particles in a given well. For low values of the forcing field F, the mutual repulsion dominates and thus we observe a larger mobility of the EPS with respect to the IBP at the same values of F and T. However, as we switch the inelasticity on, the mobility of the IPS can become lower than that corresponding to the IBP. For $F \gtrsim F_3$, μ turns out to be the same for all systems because in this regime only the forcing field F matters. In fact, the absence of minima in the total potential reduces the influence of the mutual interactions so the particles follow coherently the strong effect of the drift.

The role of the excluded volume can be highlighted by monitoring the trajectories of some specific tagged particles whose dynamics can be very representative of the evolution of the whole system. More specifically, we consider the two extremal particles, 1 and N (having labeled the rods along the drift direction from 1 to N), and the central particle, $i=N/2$.

The first particle is, on average, braked by the collisions of the preceding particles, whereas the Nth particle is pushed ahead by the pressure of those behind. Their overall behavior is expected to be qualitatively rather different from that of the central particle. In Fig. 3, we display, for $\alpha=1.0, 0.9, 0.8$, the evolution of the mean displacement of these three tracer particles from their initial position. Each displacement is normalized with respect to the displacement of the center of mass of the whole system from its initial position:

$$z_k(t) = \frac{\langle |x_k(t) - x_k(0)| \rangle}{\langle |x_{\text{c.m.}}(t) - x_{\text{c.m.}}(0)| \rangle}, \tag{5}$$

with $k=1$, $N/2$, and N. All the averages are performed over 20 independent runs.

We consider, first, the EPS for three values of the tilt F, first column of Fig. 3. For all values of F, the central particle moves with velocity very close to the center of mass velocity $v_{\text{c.m.}}$ as shown by the fact that $z_{N/2}$ stays almost pinned around the value 1. The velocities of the extremal particles, instead, are very different from $v_{\text{c.m.}}$ only during an initial transient when the system remains compact. Indeed, it is clear that in a system not yet too diluted, the motion of the first particle is frequently hindered by the others, while the motion of the last is favored. Asymptotically, the differences in the motion of rods 1, $N/2$, and N become less evident because the interactions become less effective as the packet spreads over and over. Notice, also, the asymmetry between the first and the last particle.

The major change observed when the inelasticity is turned on ($\alpha<1$) is that the velocity of the last particle displays a pronounced deviation from $v_{\text{c.m.}}$. These different behaviors are also evident by an inspection of the shapes of the instantaneous coarse grained distributions of particle positions (Fig. 4),

$$N(x,t) = \int_{x-w/2}^{x+w/2} dy \rho(y,t), \tag{6}$$

computed, in the simulations, by binning the number of particles to widths of the size of a single potential well.

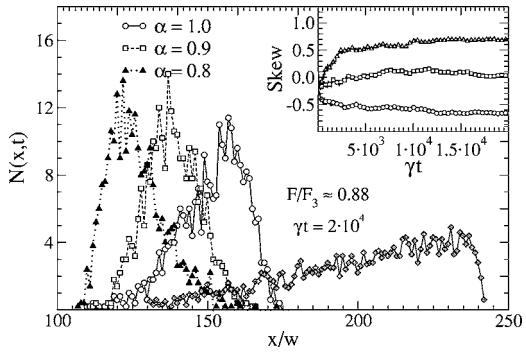

FIG. 4. Averaged number of particles, for different coefficients of restitution, as a function the dimensionless quantity x/w with $F/F_3 \simeq 0.88$ and $\gamma t = 2 \times 10^4$. The circles correspond to the elastic case ($\alpha = 1.0$) with $\sigma = 1$, while the squares and triangles to $\alpha = 0.9$ and $\alpha = 0.8$, respectively. The diamonds correspond, instead, to the elastic particles of size 10σ. The distributions extend only over few hundred wells, while the system size is much larger $L = 10^8 w$. Inset: The trend of the skewness as a function of γt in the same cases. The other parameters are the same as in Fig. 1.

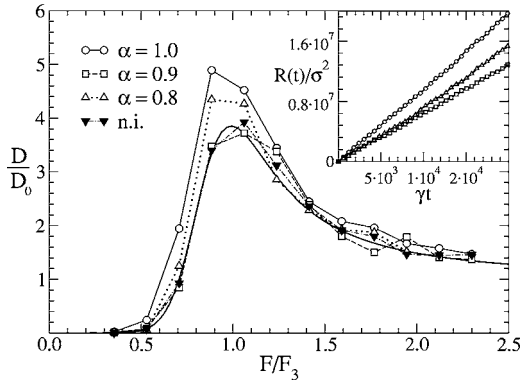

FIG. 5. The rescaled coefficient of diffusion D/D_0 ($D_0 = T/m\gamma$) as a function of F/F_3. Each point is the result of an average over ten independent runs. The circles correspond to the elastic case ($\alpha = 1.0$), while the squares and triangles to $\alpha = 0.9$ and $\alpha = 0.8$, respectively. The full line represents the theoretical result obtained by Reimann *et al.* (Ref. 22). Inset: Standard diffusion of the system rescaled spreading, $R(t)/\sigma^2$, [see Eq. (1)] with respect to the dimensionless time γt in the same cases for $F/F_3 \simeq 0.88$. The other parameters are the same as in Fig. 1.

In the EPS, the asymmetry of the packet is determined only by the excluded volume effects and, when the diameter of the rods increases from σ to 10σ, both asymmetry and drift velocity become more pronounced.

The dissipation, favoring clustering, makes the packets of the IPS more compact and, in addition, changes the direction of the asymmetry, as seen for $\alpha = 0.9$ and $\alpha = 0.8$ in Fig. 4. This effect can be quantified by means of the skewness of the particle distribution around their center of mass,

$$\mathrm{Skew}(x_1, \ldots, x_N) = \frac{1}{N} \sum_{j=1}^{N} \left(\frac{x_j - x_{\mathrm{c.m.}}}{\mathrm{rmsd}} \right)^3, \tag{7}$$

where $\mathrm{rmsd}(x_1, \ldots, x_N)$ is the standard deviation and $x_{\mathrm{c.m.}}$ the center of mass position. Positive values of Skew entail distributions with an asymmetric shape extending out toward more positive tails. Negative values are associated with distributions extending out toward more negative tails.[40] In the inset of Fig. 4, we plot the parameter Skew as a function of time for three systems with different inelasticities.

Let us consider, now, the quantity

$$D = \lim_{t \to \infty} \frac{1}{2t} R(t). \tag{8}$$

In the IBP, D is constant and corresponds to the diffusion coefficient. We have found numerically that such a behavior persists both in the EPS and IPS for all values of α we explored, as clearly indicated by the linear growth of $R(t)$ in the inset of Fig. 5.

The interactions change quantitatively the dependence of D on F; in fact, as F varies, the diffusion coefficient displays a maximum for $F \simeq F_3$ (see Fig. 5), with a behavior similar to that found by Reimann *et al.* in the IBP.[22] As α decreases, however, we observe some differences. In particular, the larger diffusivity of the EPS with respect to the IBP is basically explained by the excluded volume repulsion. At first, the diffusivity lowers as α decreases, but a further decrease of α determines a new enhancement of D (Fig. 5). Such a feature is a consequence both of the larger broadening and of the larger asymmetry of the packet occurring as the particle size grows (see Fig. 4); as a matter of fact, there is a huge increase of the diffusion since, for $F/F_3 \simeq 0.88$, we found $D/D_0 \approx 29.6$ (these data are not shown).

IV. UNDERDAMPED REGIME

When the damping force, in Eq. (2), is smaller or comparable with respect to the inertial term $m\ddot{x}$ the situation changes drastically.

At low friction, the particles can travel across several wells before being trapped in a minimum. Again, as a guide, we can use the results obtained by Risken in his thorough study on the IBP in washboard potentials, providing a full theoretical treatment of the mobility as a function of γ and temperature. Risken's theory shows the existence of two dynamical states: *locked* and *running*. At $T = 0$, a characterization of the dynamical behavior of the noninteracting system is straightforward. Indeed, for $F > F_3 = \omega_0^2$ only running states exist. When $F_1 \leqslant F \leqslant F_3$, with $F_1 = 4\gamma\pi\sqrt{mV_0}$ particles may be either locked or running depending on the initial velocity and position. This fact determines a hysteresis loop in a μ vs F diagram. When the temperature is finite, the particles can switch from one state to the other under the influence of the thermal bath. As a result, the hysteresis is suppressed and the locked-running transition occurs smoothly as a function of the tilt F, being the $\mu(T)$ curve a sigmoid in F. Only as $T \to 0^+$ the sigmoid becomes a step function whose discontinuity is located at $F_2 \simeq 3.36\gamma\sqrt{mV_0}$.

MD simulations of the underdamped regime at different values of F allowed us to determine the curve of μ as a function of the tilt, shown in Fig. 6 for the EPS ($\alpha = 1$) and the IPS with $\alpha = 0.8$ at temperatures $T = 8$ and $T = 4$.

The mobility μ appears to be roughly similar to that of the overdamped regime, but the critical F separating locked and unlocked situations lies at values lower than F_3 and depends both on γ and T. In the EPS, the mobility is rather close to the IBP value, while for the IPS the mobility is reduced, as shown explicitly in the case $\alpha = 0.8$ in Fig. 6.

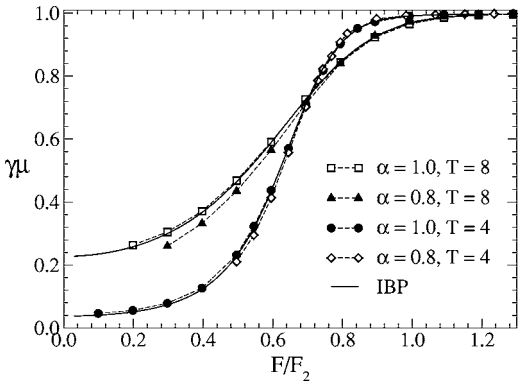

FIG. 6. Dimensionless mobility $\gamma\mu$ as a function of the external rescaled force F/F_2 for different temperatures and coefficients of restitution. The open and closed symbols refer to $T=4$ and $T=8$, respectively. The squares indicate the elastic case and the triangles the case with $\alpha=0.8$. The other parameters of the system are $\gamma=0.2t_u^{-1}$, $N=256$, $V_0=9.0$, $\sigma=1.0$, $w/\sigma=400$, and $t_{\max}=10\,000t_u$. The full line indicates the corresponding curve for the noninteracting particles, obtained via the continued fraction method by Risken.

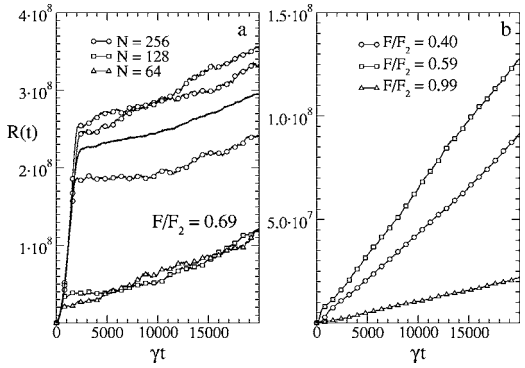

FIG. 8. Time behavior of $R(t)/\sigma^2$, (1), for the IPS with $\alpha=0.8$. Panel (a) reports three runs with $F=1.4$, $T=4$, and $N=256$ (circles), two runs with $N=128$ (squares), and two runs with $N=64$ (triangles). The full line is the average of the same quantity over ten independent runs involving $N=256$ particles. Panel (b) shows $R(t)/\sigma^2$ vs γt at temperature $T=8$ for different forces: $F=0.8$ (circles), $F=1.2$ (squares), and $F=2.0$ (triangles). The curves represent an average over five runs. The remaining parameters are the same as in Fig. 6.

While the mobility of particles interacting inelastically displays, in the underdamped regime, no peculiar behavior with respect to the IBP and EPS, their collective diffusion presents some anomalies. At low temperatures, the dynamics strongly depends on the initial conditions; the evolution of the packet is very sensitive to the tilt and exhibits a rather inhomogeneous and irregular structure. This can be readily visualized by looking at the time behavior of the coarse grained particle density $N(x,t)$ [Eq. (6)] at temperature $T=4.0$ shown in Figs. 7(a) and 7(b) for $F=1.4$ and $F=1.6$, respectively. It indicates that, for $F=1.4$, particles remain partially trapped in the well where they have been initially deposited and only a fraction of them escape acquiring a drift. For comparison we also show the corresponding behavior of $N(x,t)$ for the EPS, where the diffusion is standard. Interestingly, the inelastic distribution $N(x,t)$ corresponds to a lower mobility, but to a larger spread of the particles. Moreover, one can see that new clusters, indicated by the spikes in Fig. 7(a), spontaneously form and persist for long periods before being dissolved. Such clustering phenomena

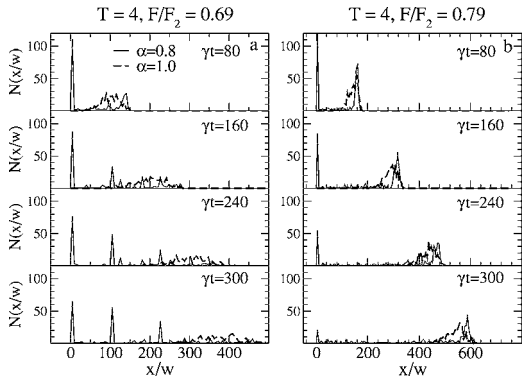

FIG. 7. Snapshots, taken a different times, of the averaged distribution $N(x,t)$ plotted as a function of the dimensionless quantity x/w, for $F=1.4$ (panel a) and $F=1.6$ (panel b), for the IPS with $\alpha=0.8$ and EPS (broken line). The remaining parameters are the same as in Fig. 6. We notice that the system size is $L=10^8w$ much larger than the well width; thus the peaks are not commensurate with the system size.

are favored by the moderate value of the tilt. The situation, instead, looks different at $F=1.6$ [see Fig. 7(b)], where the initial cluster "evaporates" earlier, and the formation of new clusters is prevented by the effects of the drift F. One observes a clear difference with respect to the behavior of the overdamped IPS illustrated in Fig. 4 showing a more compact structure of $N(x,t)$ which does not lose "debris."

Such an early stage is sufficient to determine a late collective transport characterized by an anomalous spreading. The closely packed initial configuration has deep repercussions on the late spreading, $R(t)$. This quantity, despite a very long simulation, does not appear to reach a linear or any other simple functional asymptotic dependence on time (Fig. 8). The situation described above corresponds to an early very steep growth of $R(t)$, growth that becomes slower after a characteristic time τ whose duration decreases with the tilt amplitude. As shown in Fig. 8 the vertical position of the knee strongly depends on the number of particles. By no means the $R(t)$ shows the expected linear behavior of standard diffusion. Such a feature is present only in the inelastic systems. However, when the temperature is raised, even the IPS recovers a linear behavior as seen in Fig. 8(b). The estimated diffusion coefficient is shown in Fig. 9.

The peak of D relative to the IPS is higher than the corresponding peak of the EPS. The larger value of the IPS peak can be associated with the shape of the phase-space distribution, $P(x_r,v_r)$, which is defined as the probability of finding a particle at distance x_r from the center of mass and with velocity v_r with respect to center of mass velocity $v_{\text{c.m.}}$.

The enhancement of the diffusion in the IBP is determined by the locked-running bistability, i.e., by the existence of two peaks at velocities $v=0$ and $v=F/\gamma$ in the velocity distribution. At the transition both populations are present and the center of mass velocity does not represent the most probable velocity in the system. Hence, it is clear that in this situation the variance of the velocity distribution can be very large. On the other hand, when one of the two populations becomes dominant the variance tends to decrease. The spatial part of the distribution $P(x_r,v_r)$ does not play any role in

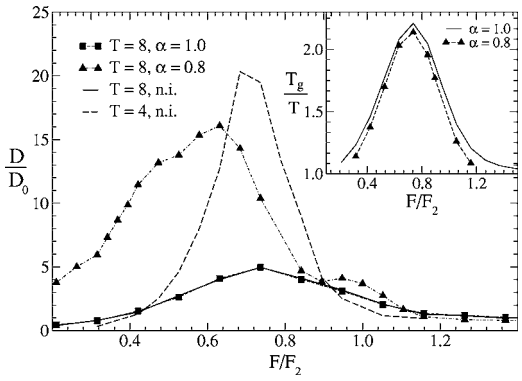

FIG. 9. Rescaled diffusion coefficient D/D_0 ($D_0=T/m\gamma$), for different coefficients of restitution, as a function of F/F_2. The D values represent averages over ten trajectories. The squares correspond to the elastic case ($\alpha=1.0$), while the triangles to $\alpha=0.8$. The temperature is $T=8.0$, the remaining parameters are the same as in Fig. 6. The dashed line indicates the result relative to the IBP at a lower temperature $T=4.0$, showing that the effect of inelastic collisions cannot be accounted for by a mere reduction of the effective temperature of the system. The inset, finally, displays the ratio between the kinetic and the heat bath temperatures.

the IBP as the x dependence of the distribution is symmetric with respect to the center of mass coordinate. The scenario changes in the interacting cases, since in one dimension (1D) the excluded volume plays a fundamental role in the dynamics. As we have seen in the inelastic case, at low temperatures the interaction was such as to lead to a fragmentation of the system and to a nonlinear behavior of the diffusion. As T increases the fragmentation decreases and $R(t)$ display a linear behavior with respect to t. In order to explain the different values of D near the peak between the IPS and the EPS, we have collected from the simulations the double histograms $P(x_r,v_r)$. The comparison is reported in Fig. 10 for drift values F near the peak. Analyzing the different behaviors of $P(x_r,v_r)$ in the various cases may help clarify the role of the interactions. In the EPS for loads $F=1.2$ and 1.4, $P(x_r,v_r)$ displays the same velocity bistability as the IBP and no spatial asymmetry and indeed the diffusion in these two systems results very similar as shown in Fig. 9. In the IPS, instead, for the same loads we observe a strong spatial asymmetry which enhances the diffusion. In the IPS, the interactions besides determining the peak of the diffusion also determine its width. From our simulations, as shown in Fig. 9, we see that the peak occurs at lower values of F with respect to the IBP and EPS and the width is much broader. This means that it is not possible to reproduce the behavior of the IPS by an appropriate choice of an effective temperature accounting for the inelasticity. A smaller temperature, in fact, would give a higher peak, but would not change the value of F at which it occurs. Moreover, the width of the peak decreases with T and fails to reproduce the observed broadening in the IPS, which is due to the interparticle interactions. In the inset of Fig. 9, we display the ratio between the kinetic temperature

$$T_g = \frac{1}{N}\sum_i \langle (v_i - v_{\text{c.m.}})^2 \rangle$$

and the heat bath temperature T. Notice that in both cases the peak occurs in correspondence of the peak of the curve D/D_0 of the elastic system and the ratio approaches, as expected, the value 1 at low and high bias F.

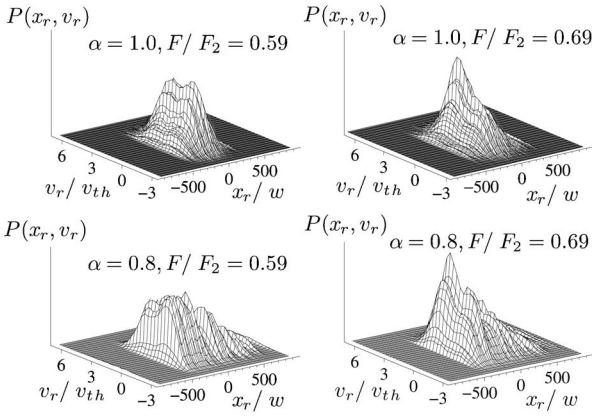

FIG. 10. Joint distribution $P(x_r,v_r)$ of position and velocity in the reference frame of the system center of mass; plots refer to force $F=1.2$ (left) and $F=1.4$ (right) in the EPS case (top) and IPS case (bottom) with $\alpha=0.8$. Independent variables have been made dimensionless through the rescaling $x/x_{\text{c.m.}}$ and v/v_{th}, with $v_{\text{th}}=\sqrt{T/m}$ the thermal velocity.

V. CONCLUSIONS

In summary, in this work we have reported a numerical study on the dynamics and the transport of an array of identical particles in an inclined washboard potential. We investigated, at several tilting F, the role of hard-core repulsive interactions among the particles on both the mobility and the spreading of the system with respect to its center of mass, indicators that are customarily used to characterize collective transport in such systems. We compared the behavior of three models involving, respectively, independent Brownian particles (IBP), elastic particles (EPS), and inelastic particles (IPS). We have found that in the high friction regime, the transport behavior of the system with interacting particles is qualitatively similar to that of the noninteracting system (IBP). Basically, the interactions do not strongly affect the mobility which remains close to the IBP value, while they modify the diffusivity that appears to be larger. This conclusion is intuitive, if we consider that μ is related the center mass velocity of the system, a quantity rather insensitive to the presence of interparticle interactions. To achieve a finer information about the structure of the collective motion, we monitored the evolution of the particle spatial distribution. Such a distribution strongly depends on the choice of the geometrical parameters and of inelasticity. This analysis shows that an initial localized packet of particle spreads differently in the inelastic system from the elastic one.

The scenario in the underdamped regime is more complex. The EPS systems, in fact, are similar to IBP analyzing either the mobility or the diffusion of the particles. The inelastic interactions practically do not affect the mobility, whereas they determine a marked change in the behavior of the diffusion at low temperatures and forces. The spreading, $R(t)$ [Eq. (1)], presents a clear two stage behavior: it increases nonlinearly in a transient regime which is then followed by a nonlinear growth, as shown in Fig. 8. At higher temperatures, however, the diffusion of the inelastic particles

exhibits a single regime, with a linear growth typical of a standard diffusion. Our study indicates, moreover, that a group of particles interacting via inelastic hard-core collisions spread over much more than elastic particles.

The mobility μ seems to be a global indicator that poorly encodes the information about the details of the interactions. On the contrary, the diffusion coefficient D is a much more representative observable being more sensitive to the presence of elastic or inelastic interactions.

We believe that in the overdamped regime, it should be possible to apply theoretical methods already employed in the study of dense molecular fluid in narrow channels,[41] whereas the treatment of the underdamped case remains more problematic. The aim of the present numerical work is, perhaps, to stimulate further investigation and new theoretical proposals.

ACKNOWLEDGMENT

Two of the authors (U.M.B.M. and F.C.) acknowledge the support of the Project Complex Systems and Many-Body Problems, COFIN-MIUR 2005, No. 2005027808.

[1] G. I. Nixon and G. W. Slater, Phys. Rev. E **53**, 4969 (1996).
[2] C. J. Olson, C. Reichhardt, B. Janko, and F. Nori, Phys. Rev. Lett. **87**, 177002 (2001).
[3] G. Barone and A. Paternò, *Physics and Applications of the Josephson Effect* (Wiley, New York, 1982).
[4] E. Hershkowitz P. Talkner, E. Pollak, and Y. Georgievskii, Surf. Sci. **421**, 73 (1999).
[5] W. Dieterich, P. Fulde, and I. Peschel, Adv. Phys. **29**, 527 (1980).
[6] F. Jülicher, A. Ajdari, and J. Prost, Rev. Mod. Phys. **69**, 1269 (1997).
[7] I. Derenyi and T. Vicsek, Phys. Rev. Lett. **75**, 374 (1995).
[8] U. Marini-Bettolo-Marconi, M. Conti, and A. Vulpiani, Europhys. Lett. **51**, 685 (2000).
[9] S. Dippel, G. G. Batrouni, and D. E. Wolf, Phys. Rev. E **54**, 6845 (1996).
[10] C. Henrique, M. A. Aguirre, A. Calvo, I. Ippolito, S. Dippel, G. G. Batrouni, and D. Bideau, Phys. Rev. E **57**, 4743 (1998).
[11] C. Ancey, P. Evesque, and P. Coussot, J. Phys. I **6**, 725 (1996).
[12] T. Poeschel, J. Phys. I **4**, 499 (1994).
[13] Z. Farkas, P. Tegzes, A. Vukics, and T. Vicsek, Phys. Rev. E **60**, 7022 (1999).
[14] H. M. Jaeger, S. R. Nagel, and R. P. Behringer, Rev. Mod. Phys. **68**, 1259 (1996).
[15] *Granular Gas Dynamics*, Lectures Notes in Physics Vol. 624, edited by T. Pöschel and N. Brilliantov (Springer-Verlag, Berlin, 2003) and references therein.
[16] L. P. Kadanoff, Rev. Mod. Phys. **71**, 435 (1999).
[17] J. Duran, *Sands Powders and Grains: An Introduction to the Physics of Granular Materials* (Springer, New York, 2000).
[18] *Granular Gases*, Lecture Notes in Physics Vol. 564, edited by T. Poeschel and S. Luding (Springer, Berlin, 2001).
[19] D. Paolotti, C. Cattuto, U. Marini-Bettolo-Marconi, and A. Puglisi, Granular Matter **5**, 75 (2003).
[20] H. Risken, *The Fokker-Planck Equation* (Springer, Berlin, 1984).
[21] W. T. Coffey, Yu. P. Kalmykov, S. V. Titov, and B. P. Mulligan, Phys. Rev. E **73**, 061101 (2006).
[22] P. Reimann, C. Van den Broeck, H. Linke, P. Hänggi, J. M. Rubi, and A. Pérez-Madrid, Phys. Rev. Lett. **87**, 010602 (2001).
[23] G. Costantini and M. Marchesoni, Europhys. Lett. **48**, 491 (1999).
[24] T. E. Harris, J. Appl. Probab. **2**, 323 (1965).
[25] C. Lutz, M. Kollmann, and C. Bechinger, Phys. Rev. Lett. **93**, 026001 (2004).
[26] A. Taloni and F. Marchesoni, Phys. Rev. Lett. **96**, 020601 (2004).
[27] F. Cecconi, A. Puglisi, U. Marini-Bettolo-Marconi, and A. Vulpiani, Phys. Rev. Lett. **90**, 064301 (2003).
[28] F. Cecconi, F. Diotallevi, U. Marini-Bettolo-Marconi, and A. Puglisi, J. Chem. Phys. **120**, 35 (2004); **121**, 5125 (2004).
[29] R. Pagnani, U. Marini-Bettolo-Marconi, and A. Puglisi, Phys. Rev. E **66**, 051304 (2002).
[30] Y. Du, H. Li, and L. P. Kadanoff, Phys. Rev. Lett. **74**, 1268 (1995).
[31] N. Sela and I. Goldhirsch, Phys. Fluids **7**, 507 (1995).
[32] D. R. M. Williams and F. C. MacKintosh, Phys. Rev. E **54**, R9 (1996).
[33] S. McNamara and W. R. Young, Phys. Fluids A **4**, 496 (1992); **5**, 34 (1993).
[34] M. Borromeo and M. Marchesoni, Phys. Lett. A **249**, 8457 (1998).
[35] M. Marchesoni and M. Borromeo, Phys. Rev. B **65**, 184101 (2002).
[36] G. G. Stokes, Trans. Cambridge Philos. Soc. **8**, 441 (1847).
[37] C. Kettner, P. Reimann, P. Hänggi, and F. Muller, Phys. Rev. E **61**, 312 (2000).
[38] D. van der Meer, K. van der Weele, and D. Lohse, Phys. Rev. E **63**, 061304 (2001).
[39] U. Marini-Bettolo-Marconi and M. Conti, Phys. Rev. E **69**, 011302 (2004).
[40] W. H. Press, S. A. Teukolsky, W. I. Vetterling, and B. P. Flannery, *Numerical Recipes in Fortran 77* (Cambridge University Press, Cambridge, UK, 1992).
[41] U. Marini-Bettolo-Marconi and P. Tarazona, J. Chem. Phys. **124**, 164901 (2006).